Angewandte Chemie

GDCh

Eine Zeitschrift der Gesellschaft Deutscher Chemiker

www.angewandte.de

Akzeptierter Artikel

Titel: An Ultraviolet Fluorophore with Narrowed Emission via Coplanar Molecular Strategy

Autoren: Xin He, Jingli Lou, Baoxi Li, Han Wang, Xiaoluo Peng, Ganggang Li, Lu Liu, Yu Huang, Nan Zheng, Longjiang Xing, Yanping Huo, Dezhi Yang, Dongge Ma, Zujin Zhao, Zhiming Wang, and Ben Zhong Tang

Zitierweise: *Angew. Chem. Int. Ed.* **2022**, e202209425

Link zur VoR: https://doi.org/10.1002/anie.202209425

WILEY-VCH

10.1002/ange.202209425

WILEY-VCH

COMMUNICATION

An Ultraviolet Fluorophore with Narrowed Emission via Coplanar Molecular Strategy

Xin He[+], Jingli Lou[+], Baoxi Li[+], Han Wang, Xiaoluo Peng, Ganggang Li, Lu Liu, Yu Huang, Nan Zheng, Longjiang Xing, Yanping Huo, Dezhi Yang, Dongge Ma, Zujin Zhao, Zhiming Wang*, and Ben Zhong Tang*

[*] X. He[+], J. Lou[+], B. Li[+], H. Wang, X. Peng, G. Li, L. Liu, Y. Huang, N. Zheng, Prof. D. Yang, Prof. D. Ma, Prof. Z. Zhao, Prof. Z. Wang
State Key Laboratory of Luminescent Materials and Devices, Guangdong Provincial Key Laboratory of Luminescence from Molecular Aggregates, Center for Aggregation-Induced Emission, AIE Institute, Guangzhou International Campus
South China University of Technology
Guangzhou 510640 (China)
E-mail: wangzhiming@scut.edu.cn
Prof. B. Z. Tang
Shenzhen Institute of Aggregate Science and Technology, School of Science and Engineering
The Chinese University of Hong Kong, Shenzhen
Shenzhen 518172 (China)
E-mail: tangbenz@cuhk.edu.cn
L. Xing, Prof. Y. Huo
School of Chemical Engineering & Light Industry
Guangdong University of Technology
Guangzhou 510006 (China)

[+] These authors contributed equally to this work.

Supporting information for this article is given via a link at the end of the document.

Abstract: Narrowband emitting fluorophores exhibit immense potentials for organic light-emitting diodes (OLEDs) with high color purity. However, it's still hard to simultaneously realize short-wavelength ultraviolet (UV) or near ultraviolet emission (NUV) while maintaining a narrowed full width at half maximum (FWHM) value, and rare work focus on such challenging pursuit. Herein, an ingenious synthetic method was devised to achieve emitters with coplanar structure. 11-(4,6-diphenyl-1,3,5-triazin-2-yl)indolo[3,2,1-*jk*]carbazole (ICZ-TAZ) was designed to realize narrowed UV emission both in photoluminescence (PL) and electroluminescence (EL) which benefited from the suppression of vibronic coupling. UV/NUV OLEDs based on ICZ-TAZ achieve external quantum efficiency (EQE) maximums of 3.26% peaks @ 388 nm and 4.02 % peaks @ 406 nm with small FWHM of 32 nm and 46 nm, respectively, corresponding with reduced efficiency roll-off at luminance of 100 cd m^{-2}.

*O*rganic light emitting diodes (OLEDs) has been developed expeditiously over the last three decades[1]. Recently, ultraviolet (UV) or near ultraviolet (NUV) emission of organic fluorescent compounds attracted much attention for their profitable characters[2]. The short-wavelength emission can not only fulfill the visible light region, but also provides wider applications as the light source for all visible colors and other fields[3] such as sterilization, sensing and high-density information storage. Traditional electron donor-acceptor (D-A) type fluorophores have abundant building blocks to regulate the highest occupied molecular orbital (HOMO) and the lowest unoccupied molecular orbital (LUMO) levels to cover the emitting region from UV to infrared. However, the D-A molecules, especially for the thermally activated delayed fluorescence (TADF) emitters with twisted structure, suffered from broadening emission with full width of half maximum (FWHM) up to 70-100 nm which mainly attributed to the structural relaxation and vibronic coupling of the long-ranged charge transfer (CT) excited states[4]. Particularly, extremely rare UV TADF-based OLEDs were reported except for CZ-MPS[4e], which contains an optimized LUMO energy level to acquire the UV emission. To overcome the predicament, polycyclic aromatic hydrocarbons (PAHs) with rigid planar structure were exploited as efficient method suppressing the structural dynamics driven by electronic changes[5]. Moreover, series of PAHs utilized opposite resonance effect of different atoms to realize the separation of HOMO and LUMO, finally achieving desirable narrow FWHM below 20 nm of the enhanced emission through multiple resonance (MR) effect[6]. These short-range CT states also minimized exchange interactions which promoted reverse intersystem crossing (RISC) process to arise TADF. Thus, the MR-TADF emitters could harvest triplets and achieve ideal deep-blue device performances with external quantum efficiency (EQE) over 30%. Nevertheless, because that the opposite resonance effects among atoms are relatively stationary, extremely rare MR emitters could reach UV/NUV emitting region. Therefore, there still remains pressing challenges to simultaneously realize short-wavelength emission while maintaining a narrowed FWHM value.

Besides MR-based emitters, another promising way to narrow the emission and increase the excited state energy at the same time is to construct coplanar structure which helps reducing the vibronic coupling. Pioneer workers reported coplanar molecules which exploited acridine-like fused donor to achieve rigid structure and the corresponding narrowed emission[7]. However, the incomplete conjugation of quaternary carbon in the acridine-like donor units and the restricted rotation between D/A units lead to a certain degree of spectral broadening. Hence, suitable molecular structure and design strategy are imperative for the simultaneous implementation of more narrowed and blue-shifted emission. Indolo[3,2,1-*jk*]carbazole (ICZ) is found to be a

10.1002/ange.202209425

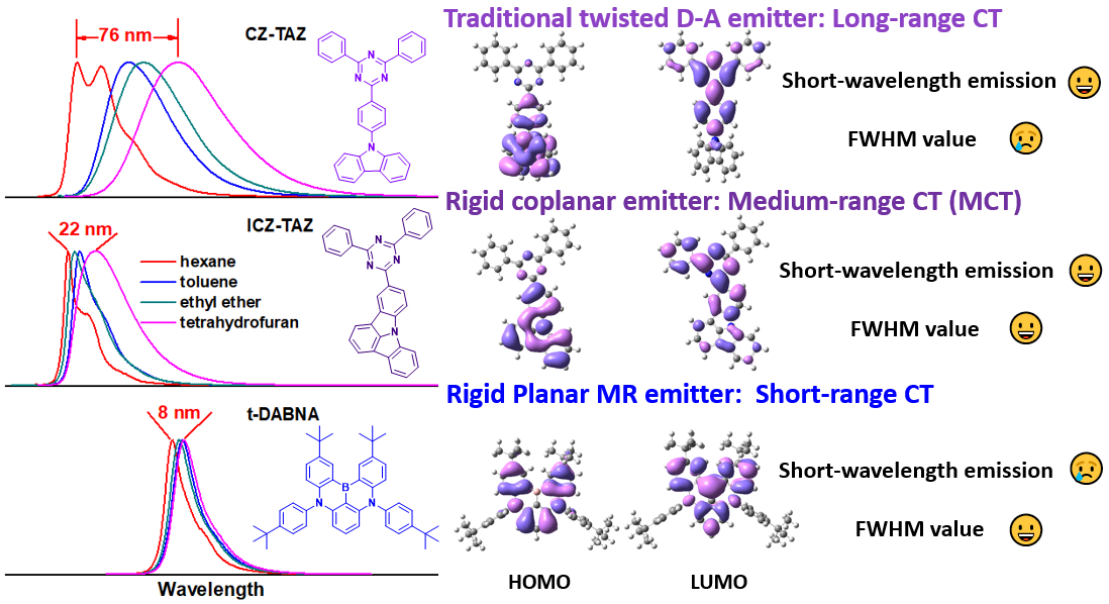

Figure 1. Illustration of design strategy of coplanar emitter ICZ-TAZ: contrastive study on molecular structure, solvatochromism effect and HOMO/LUMO distributions of ICZ-TAZ, CZ-TAZ and t-DABNA.

burgeoning electron donor with planar structure which developed in recent years. In 2020, ICZ derivative named tDIDCz was reported with axial symmetry planar molecular structure[8], which exhibited strong NUV electroluminescence (EL) emission with extremely narrow FWHM. Moreover, a series of structural optimization of ICZ were carried out, which successfully raised the EL performances but undesirably red-shifted the emitting region or broadened the spectra[5b-d, 9]. It's noteworthy that the HOMO of tDIDCz is rather low of -5.98 eV as reported, which implied that ICZ unit may be qualified for short-wavelength emission construction. Differ from widely used donor moieties such as diphenylamine (DPA), carbazole (CZ) and 9,9-dimethyl-9,10-dihydroacridine (DMAC), ICZ lacks active secondary amine to directly participate in Buchwald-Hartwig coupling reactions. So, it's crucial to develop an appropriate substituting method for ICZ to realize both narrowed and UV/NUV emission. To address the aforementioned issue, we carried out a shortcut to in situ generate ICZ to acquire its coplanar derivatives. The resulting 11-(4,6-diphenyl-1,3,5-triazin-2-yl)indolo[3,2,1-*jk*]carbazole (ICZ-TAZ) shows rigid coplanar structure and emits UV emission with narrowed FWHM. Further, efficient single-doped UV/NUV devices based on ICZ-TAZ were successfully fabricated.

The molecular structure of ICZ-TAZ is shown in Figure 2a. ICZ-TAZ was obtained from a one-shut reaction named double-halide cyclized coupling (DHCC) reaction as shown in Scheme S1, which immensely simplify the synthesis complexity and reduced the corresponding costs to obtain fused planar structure. After introducing single sigma bond "lock" to the well-studied D-A type emitter CZ-TAZ [7a, 10], the original planar acceptor TAZ segment is combined with the newly generated rigid donor ICZ moiety to give the coplanar structure of ICZ-TAZ. To further confirm the correctness of the structure and study the molecular configuration, the single crystal of ICZ-TAZ was cultured and analyzed as shown in Figure 2c. ICZ-TAZ entirely shows manifested coplanar structure with one of the benzene rings of TAZ moiety slightly twisted (13.02°). The strong intramolecular hydrogen bonds (2.489-2.542 Å) in TAZ directly contribute to the entire planarity of ICZ-TAZ. For comparison, the ground state geometry is also optimized via density functional theory (DFT) at M062X/6-31(d, p) level (Figure 2b). ICZ-TAZ shows a paper-like planar structure (Figure S3), which is consistent with the configuration obtained in the crystal. When aggregated, such flat structure may easily form puissant homogeneous or/and heterogeneous intermolecular interactions. As shown in Figure 2d-e, the packing structure of ICZ-TAZ crystal displays an obvious face-to-face *π-π* interaction with a short distance of 3.553 Å. Moreover, the overlap between the planes is quite large (Figure 2f) indicating that such *π-π* interaction is extremely strong.

The photophysics properties of ICZ-TAZ were preliminary investigated in dilute toluene with a concentration of 10^{-5} M. ICZ-TAZ shows a sharp absorption peak at 371 nm with high molar absorbance coefficient of 24106 M^{-1} cm^{-1}, which is identified and ascribed to be the *π-π** absorption of the conjugated skeleton of the coplanar structure (Figure 3a). With wide optical gap of 3.22 eV, ICZ-TAZ exhibits strong UV emission with peak at 381 nm with tiny Stokes shift of 635 cm^{-1}, which implies that small structural relaxation occurred upon photoexcitation for the rigid structure. Particularly, benefited from the suppression of vibronic coupling, ICZ-TAZ shows a desirable competitive narrow FWHM of 25 nm (0.21 eV) which is consistent with the original design intention. Additionally, the Commission Internationale de L'Eclairage (CIE) y value is as low as 0.015 incorporating its short-wavelength and narrowed emission. The solvatochromic effect was tested in various solvents with diverse polarities to further analyze the excited-state properties (Figure 3d). The emission peaks of ICZ-TAZ gradually red-shift from 372 to 394 nm as the solvent polarity increases from *n*-hexane to tetrahydrofuran (THF), accompanied by the broadening of spectra with FWHM from 21 nm (0.18 eV) to 45 nm (0.36 eV). After polarized in THF, the hydrogen bonds interactions between ICZ and TAZ fragments are weakened and leads to a certain degree of torsion of the entire coplanar structure, which finally led to the increase of vibrational energy levels and brought out the broadened spectra in high-polarity solvents. Differ from traditional twisted electron D-A type molecule CZ-TAZ (red shift: 76 nm) with long-ranged CT state, ICZ-TAZ shows quite reduced red-shifts (22 nm) and narrowed FWHM (Figure S7), which mainly owes to the structural rigidity to restrict the relaxation of excited states. Moreover, the shortened

10.1002/ange.202209425

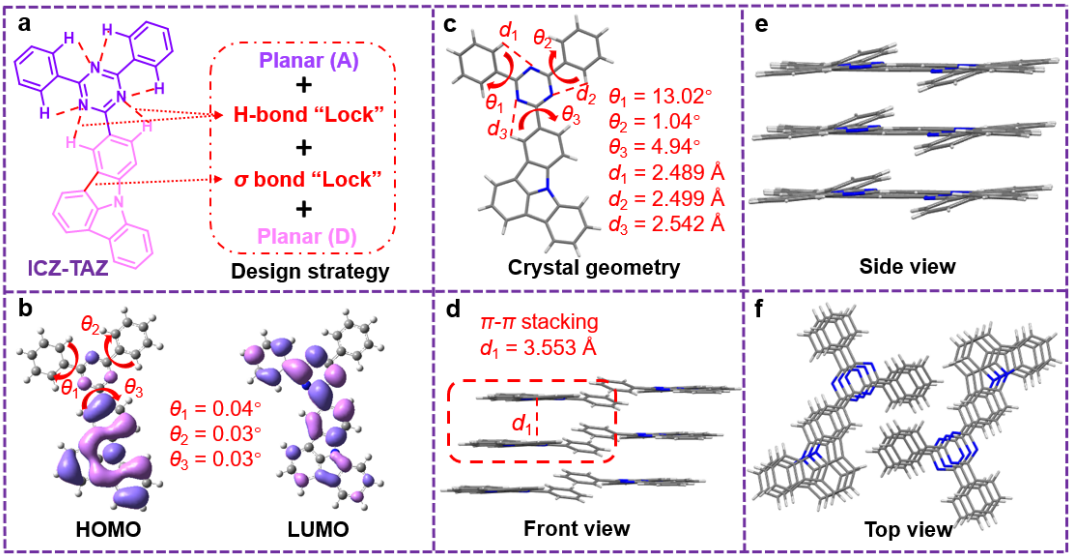

Figure 2. a) Chemical structure and coplanar molecular design for ICZ-TAZ. b) Geometry and HOMO/LUMO of S_0 state optimized by DFT. c) Crystal structure of ICZ-TAZ and its three views (d-f) of molecular packing.

distance between HOMO and LUMO also affects when ICZ moiety is in situ synthesized to planarized the structure which results in the wider distribution and larger overlap of HOMO and LUMO. Thus, ICZ-TAZ could be described as coplanarity induced medium-ranged CT (MCT) state when compared with typical blue MR-TADF emitter t-DABNA with absolute planar structure and short-ranged CT state originated from distinct opposite resonance effects (Figure 1). Further, low-temperature photoluminescence (PL) spectroscopy in toluene was measured to estimate the energy level of the lowest triplet state (T_1) (Figure 3b). The T_1 of ICZ-TAZ is 2.86 eV which is obtained from the emission onset of phosphorescence spectrum with a delay scale of 10 ms, and the ΔE_{ST} is therefore calculated to be 0.50 eV (S_1 is 3.36 eV obtained from the spectrum at 77 K). ICZ-TAZ shows a completed single-exponential decay in deoxygenated toluene within time ranged of 100 ns and the lifetime is fitted to be 2.34 ns (Figure 3c) without delayed component, indicating that no TADF arise with such large ΔE_{ST}. Generally, the rigid structures of emitters are usually accompanied by high photoluminescence quantum efficiency (PLQY) which help restraining the energy loss of vibration or/and rotation. However, ICZ-TAZ gains a relatively low PLQY of 52% in deoxygenated toluene. Considering the great rigidity and small Stokes shift of ICZ-TAZ, a competitive intersystem crossing (ISC) process may exist to partially convert singlets to triplets without return. The theoretical calculation of excited states also illustrates that there are available triplet states with small energy differences suitable for the lowest singlet state (S_1) to transform (Figure S4).

Further, ICZ-TAZ was dispersed in bis[2-(diphenylphosphino)-phenyl]ether oxide (DPEPO) or 2,8-bis(diphenylphosphoryl)dibenzo[b,d]furan (PPF) with various concentrations (1, 10, 20 and 30 wt%) to form the host-guest solid films. The absorption of ICZ-TAZ exhibited good spectral overlap with the emission of DPEPO and PPF (Figure S20), indicating that the Förster resonance energy transfer (FRET) from the host to the guest emitter could be efficient. The excitation wavelength for the films is 290 nm according to the comparison of the absorption spectra which could excite the guest as well as the host materials (Figure S9). Both 1 wt% DPEPO and PPF films exhibit UV emission with narrowed FWHM of 46 nm and 43 nm, respectively, which are consistent with the PL spectra in THF solution sharing similar emission peaks and FWHM (Figure S10). This suggests that the similar high polarities of the matrixes primarily widened the emission of ICZ-TAZ in its low-concentration doped films. The PL spectra were further broadened and red-shifted after the doping concentration raised, attributing to the enhanced homogeneous and heterogeneous intermolecular interactions originated from the planar structure of ICZ-TAZ. Calculated from the low temperature spectra, the doped films maintain high ΔE_{ST} values even if the fluorescence spectra red-shift as the concentrations increase. The doping films with 1 wt% and 10 wt% ICZ-TAZ in PPF possess the highest PLQY of 49.2% and 47.8% among the fabricated films, which further contribute to the better EL performances. Then transient PL decays of these films were measured with time range of both nanoseconds and microseconds at their emission maximum (Figure S15 and S16, Table S2). Majority of the films were found to involve obvious delayed components with lifetimes of microseconds together with the IRF signal except for the doped film with 1 wt% ICZ-TAZ in DPEPO. Considering the absence of TADF for ICZ-TAZ in its solitary states and sustained large ΔE_{ST} in host-guest films (Figure S13 and S14), the delayed components may originate from host-guest interactions. Moreover, the relative intensity of the spectrum for DPEPO: 1 wt% ICZ-TAZ film at long wavelength obviously increased in vacuum compared with other doping films, implying the red-shifted component is sensitive to oxygen which is different from its peaked emission (Figure 3e, Figure S11 and S12). Then transient PL decay at estimated wavelength of 490 nm preliminarily found obvious delayed component compared with the IRF signal (Figure 3f). Further, these two emitting components were approximately separated by time-resolved spectra (Figure S17d) to figure out a delayed emission with more accurate peak at 460 nm. Then temperature-dependent PL decay at 460 nm was carried out to find that the ratio of delayed component gradually increased with improved temperatures, which definitely proved the TADF features (Figure S17f). Then, 370 nm wavelength light source was introduced to merely activate the dopant ICZ-TAZ for comparison, and there is no delayed signal found at neither 460 nm nor 395 nm (Figure S17-b). This indicates that the TADF at long wavelength originated from the process with participation of the hosts DPEPO/PPF, i.e. exciplex-

10.1002/ange.202209425

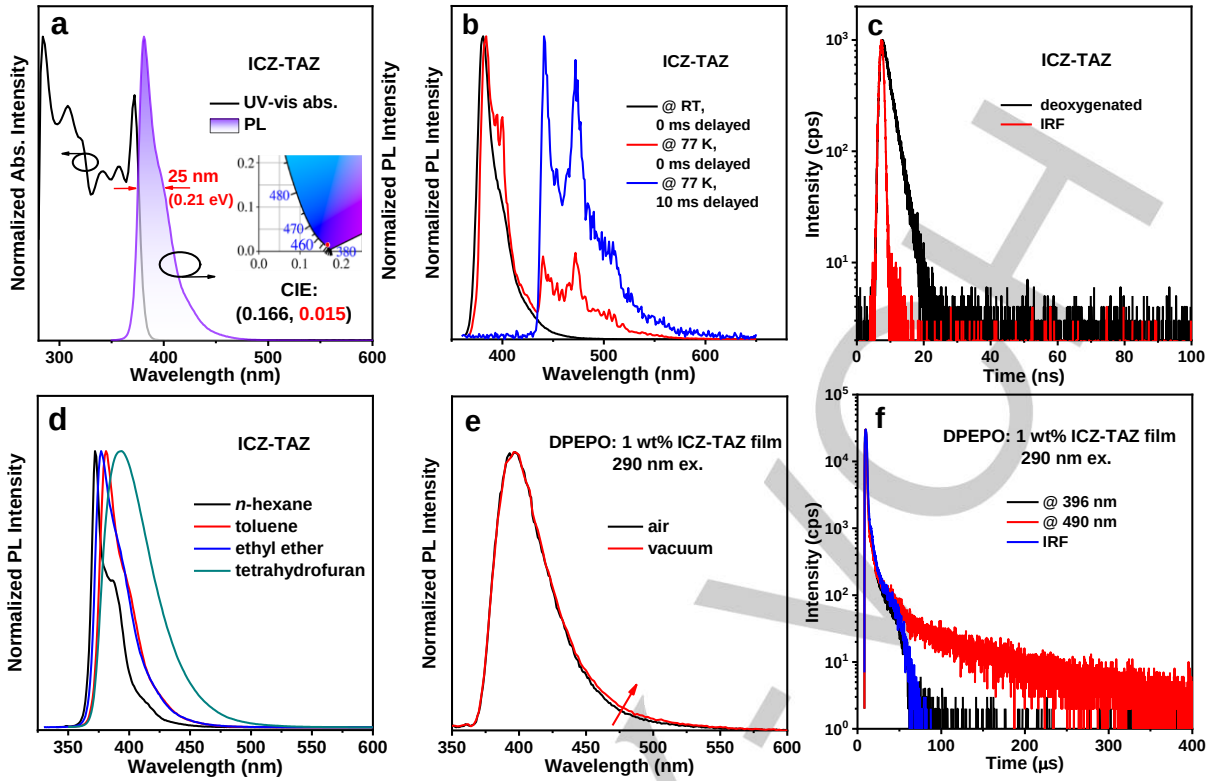

Figure 3. a) UV-vis absorption, PL spectra (Inset: corresponding CIE image) and b) low-temperature PL spectra under various condition of ICZ-TAZ in dilute toluene (10^{-5} M). c) Transient PL decay of ICZ-TAZ dilute toluene solution (10^{-5} M) with a time range of 100 ns. d) PL spectra in various solutions. e) PL spectra of DPEPO: 1 wt% ICZ-TAZ film under air and vacuum condition. f) Transient PL decays of DPEPO: 1 wt% ICZ-TAZ film at different wavelengths.

TADF in this case. The high-laid T_1 and strong interaction tendency of planar ICZ-TAZ promoted the partial exciplex formation with the host DPEPO, which was usually inclined not to form exciplex because of their high triplet energy[11]. Consequently, the observed TADF lifetimes for all the doped films come from the mixed spectra of solitary ICZ-TAZ and exciplex emission. Afterwards, the PL spectrum of DPEPO: 1 wt% ICZ-TAZ film was also simulated (Figure S17e). To achieve high goodness of fit, an additional shoulder emission peak of vibronic structure was involved which was also clearly observed in its PL spectra in solutions. The relevant photophysics data were summarized in Table S2.

The electrochemical property for ICZ-TAZ was investigated by cyclic voltammetry (CV) measurements. As shown in Figure S18, based on the onsets of the oxidation and reduction curves (versus ferrocene/ferrocenium redox couple), the corresponding values of ionization potential (IP_{CV}) and electron affinities (EA_{CV}) of ICZ-TAZ were calculated to be 5.71 eV and 2.79 eV, respectively, which derived from the donor ICZ and acceptor TAZ fragments. Thermal properties were evaluated by thermal gravity analysis (TGA) and differential scanning calorimetry (DSC) measurements (Figure S19). Benefited from the rigid molecular structure, ICZ-TAZ showed sufficiently high decomposition temperatures (T_d, corresponding to 5 % weight loss) of 411 °C which enable the emitter to be qualified for OLED manufacturing via a vacuum thermal deposition process. ICZ-TAZ also exhibited excellent morphological stability with high glass transition temperatures (T_g) of 174 °C and melting point (T_m) of 278 °C. The sterling thermal characters of ICZ-TAZ build solid foundation for further device fabricating.

Device evaluation was then carried out by doping ICZ-TAZ in DPEPO or PPF, which were selected as suitable host matrix for OLEDs because of their high triplet energy to prevent energy back-transfer and appropriate HOMO/LUMO energy levels. After meticulous optimization, the final single doped devices were fabricated with the configuration of ITO/HATCN (5 nm)/ TAPC (40 nm)/ mCP (10 nm)/DPEPO or PPF: x wt% ICZ-TAZ (20 nm)/DPEPO or PPF (5 nm)/TmPyPb (40 nm)/LiF (1 nm)/Al (x = 1, 10, 20 and 30), where ITO and Al served as anode and cathode, respectively; dipyrazino(2,3-f:2',3'-h)-quinoxaline-2,3,6,7,10,11-hexacarbonitrile (HATCN), di-[4-(*N,N*-ditolyl-amino)-phenyl] cyclohexane (TAPC) and N,N'-dicarbazolyl-3,5-benzene (mCP) were applied as the hole injecting layer, hole transporting layer and exciton blocking layer, respectively; DPEPO or PPF, 1,3,5-tri(*m*-pyrid-3-yl-phenyl)benzene (TmPyPb) and LiF acted as exciton blocking layer, electron transporting layer and electron injecting layer, respectively. The energy level diagram of the devices, molecular structures of the related materials as well as detailed EL characteristics of PPF and DPEPO hosted devices are provided in Figure 4 and Figure S23 and the key parameters are summarized in Table 1 and Table S3, respectively.

Both PPF- (Device 1-4) and DPEPO-based (Device 5-8) devices were almost turned on below 4 V, indicating that the injected carriers transported easily between optimized functional and emitting layers. All devices radiate stable UV to NUV light with EL peaks from 386 nm to 418 nm with narrowed FWHM of 32 nm to 58 nm. The EL peaks red-shifted and the corresponding FWHM raised as the doping concentration increased, which mainly attributed to the strong intermolecular interactions of planar ICZ-TAZ and the formation of exciplex. The high polarity of DPEPO and PPF also influences although ICZ-TAZ exhibits weak solvatochromism characters. Compared with DPEPO, PPF-based doped devices presented superior performances which may benefited from the more matching energy levels between

10.1002/ange.202209425

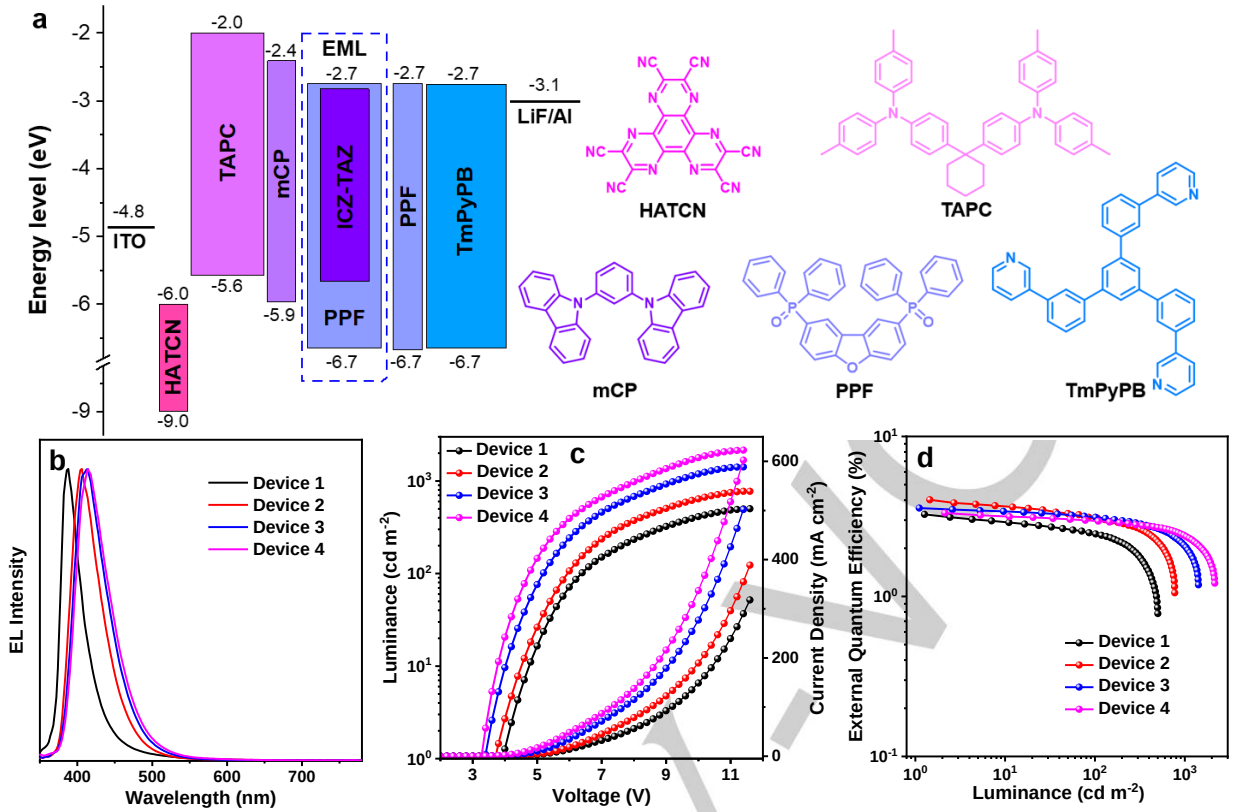

Figure 4. a) The energy level diagram of the PPF-based devices and the chemical structures of the functional layers. b) The EL spectra, c) the Luminance-voltage-current density curves and d) the EQE versus luminance curves of devices 1-4.

different layers. The best results of these devices were achieved at 1 wt% (device 1) and 10 wt% (device 2) doping concentrations in PPF host (Figure 4). Device 1 showed UV emission with EL peak of 388 nm and an ideal FWHM of 32 nm (0.26 eV), which is similar to the spectrum of the DPEPO-based device at same doping concentration. The EL spectra were blue-shifted and narrowed in a certain degree when compared with the PL spectra of the doped films with the same concentration of 1 wt%, which could be explained as the influence of the different generation and deactivation pathways of the excitons. Inspiringly, device 1 achieve a high EQE_{max} of 3.26% along with a relatively small efficiency roll-off at 100 cd m^{-2} [4e, 5c-d, 8, 9a-c] in spite of the low spectral sensitivity in such emitting region. It's noticeable that the CIEy value of device 1 is unanticipated high of 0.069, which attributed to the obvious trailing emission originated from exciplex. As the concentration was raised to 10 wt% to give device 2, the EL peak red-shifted to NUV region of 406 nm with an increased FWHM of 46 nm (0.34 eV) which caused by the enhanced intermolecular interactions of the dopants. Moreover, the CIE of device 2 is (0.162, 0.037), which fully satisfied the demands on y value of Rec. 2020 recommended by the International Telecommunication Union Radiocommunication Sector (ITUR). Device 2 obtained a highest EQE_{max} of 4.02% among the optimized doped devices, accompanied with a maximum current efficiency (CE_{max}) of 0.76 cd/A and a maximum power efficiency (PE_{max}) of 0.63 lm/W. Combined with the PLQY of PPF: 1 wt% (PLQY = 49.2%) and 10 wt% (PLQY = 47.8%) ICZ-TAZ films, the exciton utilization efficiencies were calculated to be 33.1% and 42.1%, respectively, when the out-coupling efficiency of these violet OLEDs is regarded as 20% considering the emitting region and the moderate dipole orientation simulated in Figure S22. The exciplex-TADF, as previously proved, mainly contributed to the triplets harvesting. To the best of our knowledge, the remarkable narrowed FWHM of 32 nm and the decent EQE value of 3.26%

Table 1. Electroluminescence data of ICZ-TAZ doped devices with PPF host.

Device	V_{on} [a] (V)	L_{max} [b] (cd m^{-2})	PE_{max} [c] (lm W^{-1})	CE_{max} [d] (cd A^{-1})	EQE [e] (%)			λ_{max} [f] (nm)	FWHM [g] (nm/eV)	CIE [h] (x, y)
					Max	@100 cd m^{-2}	@1000 cd m^{-2}			
1	4.0	502	0.52	0.66	3.26	2.46	---	388	32/0.26	(0.172, 0.069)
2	3.8	774	0.63	0.76	4.02	3.09	---	406	46/0.34	(0.162, 0.037)
3	3.4	1419	0.79	0.85	3.56	3.13	2.10	414	52/0.36	(0.159, 0.040)
4	3.4	2155	0.91	0.98	3.32	2.95	2.41	414	52/0.37	(0.161, 0.047)

[a] V_{on}: Turn on voltage at 1 cd m^{-2}; [b] L_{max}: Maximum luminance; [c] PE_{max}: Maximum power efficiency; [d] CE_{max}: Maximum current efficiency; [e] EQE: External quantum efficiency; [f] λ_{max}: Electroluminescence peaks of the EL spectra; [g] FWHM: Full width at half maximum of the spectra given in wavelength and energy; [h] CIE: Commission Internationale de L'Eclairage coordinates at 100 cd m^{-2}.

10.1002/ange.202209425

with reduced efficiency roll-off are among the best results of UV OLEDs.

In conclusion, we develop an artful convenient method towards molecular design with coplanar structure, and finally obtain ICZ-TAZ with in situ introduction of ICZ unit. The rigid skeleton and comparative medium-ranged charge transfer state enables ICZ-TAZ to possess significant narrowed emission, meanwhile, the deep HOMO energy level of ICZ helps to simultaneously achieve ideal short-wavelength emission. ICZ-TAZ shows narrowed UV emission in solution with small FWHM of 25 nm and weak solvatochromic effect. Further analysis on its host-guest doped film finds out partial exciplex-TADF formation which helps harvesting triplet exciton and broadens the spectra at the same time. Finally, the single doped UV- and NUV-OLED based on ICZ-TAZ provides high maximum EQEs of 3.26% and 4.02% with small efficiency roll-off at 100 cd m^{-2}, accompanied by the satisfactory FWHM of 32 nm and 46 nm with CIE coordinates of (0.172, 0.069) and (0.162, 0.037) which EL peak at 388 nm and 406 nm, respectively. The appreciable results obtained in this work demonstrates promising potential for coplanar construction in high performance emitters, which concurrently paves a new way to develop efficient UV/NUV OLEDs with high color purity.

Acknowledgements

We are grateful for National Natural Science Foundation of China (21788102, 21975077), the National Key R&D Program of China (Intergovernmental cooperation project, 2017YFE0132200), Natural Science Foundation of Guangdong Province (2022B1515020084) and Fund of Guangdong Provincial Key Laboratory of Luminescence from Molecular Aggregates (2019B030301003). Open Research Project of Military Logistics Support Department (BLB19J008), the Independent research project of State Key Lab of Luminescent Materials and Devices (SCUT) (Skllmd-2022-01).

Keywords: coplanar structrue • narrowband emission • ultraviolet emitter • organic light-emitting diodes • organic electronics

[1] a) C. W. Tang, S. A. VanSlyke, *Appl. Phys. Lett.* **1987**, *51*, 913; b) M. A. Baldo, D. O'Brien, Y. You, A. Shoustikov, S. Sibley, M. Thompson, S. R. Forrest, *Nature* **1998**, *395*, 151; c) X. Ai, E. W. Evans, S. Dong, A. J. Gillett, H. Guo, Y. Chen, T. J. H. Hele, R. H. Friend, F. Li, *Nature* **2018**, *563*, 536; d) Y. Xu, P. Xu, D. Hu, Y. Ma, *Chem. Soc. Rev.* **2021**, *50*, 1030; e) X. Tang, L.-S. Cui, H.-C. Li, A. J. Gillett, F. Auras, Y.-K. Qu, C. Zhong, S. T. E. Jones, Z.-Q. Jiang, R. H. Friend, L.-S. Liao, *Nat. Mater.* **2020**, *19*, 1332; f) X. Guo, P. Yuan, J. Fan, X. Qiao, D. Yang, Y. Dai, Q. Sun, A. Qin, B. Z. Tang, D. Ma, *Adv. Mater.* **2021**, *33*, 2006953.

[2] a) M. Shimizu, T. Sakurai, *Aggregate* **2022**, *3*, e144; b) M. Chen, Y. Liao, Y. Lin, T. Xu, W. Lan, B. Wei, Y. Yuan, D. Li, X. Zhang, *J. Mater. Chem. C* **2020**, *8*, 14665. c) H. Zhang, G. Li, X. Guo, K. Zhang, B. Zhang, X. Guo, Y. Li, J. Fan, Z. Wang, D. Ma, B. Z. Tang, *Angew. Chem. Int. Ed.* **2021**, *60*, 22241; d) J. Chen, H. Liu, J. Guo, J. Wang, N. Qiu, S. Xiao, J. Chi, D. Yang, D. Ma, Z. Zhao, B. Z. Tang, *Angew. Chem. Int. Ed.* **2022**, *61*, e202116810; e) Y. Zheng, Z. Wang, X. Wang, J. Li, X. J. Feng, G. He, Z. Zhao, H. Lu, *ACS Appl. Electron. Mater.* **2021**, *3*, 422; f) P. H, C. Lin, D. Ma, A. Qin, B. Z. Tang, *ACS Appl. Mater. Interfaces* **2020**, *12*, 46366.

[3] a) J. Chen, S. Loeb, J.-H. Kim, *Environ. Sci. Water Res. Tech.* **2017**, *3*, 18;. b) E. Espid, F. Taghipour, *Crit. Rev. Solid State Mater. Sci.* **2017**, *42*, 416; c) H. V. Santen, J. H. M. Neijzen, *Jpn. J. Appl. Phys.* **2003**, *42*, 1110.

[4] a) H. Uoyama, K. Goushi, K. Shizu, H. Nomura, C. Adachi, *Nature* **2012**, *492*, 234; b) Q. Zhang, B. Li, S. Huang, H. Nomura, H. Tanaka, C. Adachi, *Nat. Photonics* **2014**, *8*, 326; c) Q. Zhang, J. Li, K. Shizu, S. Huang, S. Hirata, H. Miyazaki, C. Adachi, *J. Am. Chem. Soc.* **2012**, *134*, 14706; d) S. Wang, X. Yan, Z. Cheng, H. Zhang, Y. Liu, Y. Wang, *Angew. Chem. Int. Ed.* **2015**, *54*, 13068; e) Y. Luo, S. Li, Y. Zhao, C. Li, Z. Pang, Y. Huang, M. Yang, L. Zhou, X. Zheng, X. Pu, Z. Lu, *Adv. Mater.* **2020**, *32*, 2001248; f). C.-C. Peng, S.-Y. Yang, H.-C. Li, G.-H. Xie, L.-S. Cui, S.-N. Zou, C. Poriel, Z.-Q. Jiang, L.-S. Liao, *Adv. Mater*. **2020**, *32*, 2003885; g) H. J. Kim, H. Kang, J.-E Jeong, S. H. Park, C. W. Koh, C. W. Kim, H. Y. Woo, M. J. Cho, S. Park, D. H. Choi, *Adv. Funct. Mater.* **2021**, *31*, 2102588.

[5] a) J. Wagner, P. Z. Crocomo, M. A. Kochman, A. Kubas, P. Data, M. Lindner, *Angew. Chem. Int. Ed.* **2022**, e202202232; b) X. Zeng, X. Wang, Y. Zhang, G. Meng, J. Wei, Z. Liu, X. Jia, G. Li, L. Duan, D. Zhang, *Angew. Chem. Int. Ed.* **2022**, *61*, e202117181; c) J. Wei, C. Zhang, D. Zhang, Y. Zhang, Z. Liu, Z. Li, G. Yu, L. Duan, *Angew. Chem. Int. Ed.* **2021**, *60*, 12269; d) V. V. Patil, J. Lim, J. Y. Lee, *ACS Appl. Mater. Interfaces* **2021**, *13*, 14440.

[6] a) T. Hatakeyama, K. Shiren, K. Nakajima, S. Nomura, S. Nakatsuka, K. Kinoshita, J. Ni, Y. Ono, T. Ikuta, *Adv. Mater.* **2016**, *28*, 2777; b) Y. Kondo, K. Yoshiura, S. Kitera, H. Nishi, S. Oda, H. Gotoh, Y. Sasada, M. Yanai, T. Hatakeyama, *Nat. Photonics* **2019**, *13*, 678; c) S. O. Jeon, K. H. Lee, J. S. Kim, S.-G. Ihn, Y. S. Chung, J. W. Kim, H. Lee, S. Kim, H. Choi, J. Y. Lee, *Nat. Photonics* **2021**, *15*, 208; d) X. Liang, Z.-P. Yan, H.-B. Han, Z.-G. Wu, Y.-X. Zheng, H. Meng, J.-L. Zuo, W. Huang, *Angew. Chem. Int. Ed.* **2018,** *57*, 11316; e) Y. Xu, C. Li, Z. Li, J. Wang, J. Xue, Q. Wang, X. Cai, Y. Wang, *CCS Chem.* **2021**, *3*, 2077; f) F. Liu, Z. Cheng, Y. Jiang, L. Gao, H. Liu, Z. Feng, P. Lu, W. Yang, *Angew. Chem. Int. Ed.* **2022**, *61*, e202116927; g) S. M. Suresh, E. Duda, D. Hall, Z. Yao, S. Bagnich, A. M. Z. Slawin, H. Bässler, D. Beljonne, M. Buck, Y. Olivier, A. Köhler, E. Zysman-Colman, *J. Am. Chem. Soc.* **2020**, *142*, 6588; h) Y. Qi, W. Ning, Y. Zou, X. Cao, S. Gong, C. Yang, *Adv. Funct. Mater.* **2021**, *31*, 2102017; i) Y. Liu, X. Xiao, Y. Ran, Z. Bin, J. You, *Chem. Sci*. **2021**, *12*, 9408; j) X. Li, Y.-Z. Shi, K. Wang, M. Zhang, C.-J. Zheng, D.-M. Sun, G.-L. Dai, X.-C. Fan, D.-Q. Wang, W. Liu, Y.-Q. Li, J. Yu, X.-M. Ou, C. Adachi, X.-H. Zhang, *ACS Appl. Mater. Interfaces* **2019**, *11*, 13472.

[7] a) X.-K. Chen, Y. Tsuchiya, Y. Ishikawa, C. Zhong, C. Adachi, J.-L. Brédas, *Adv. Mater.* **2017**, *29*, 1702767; b) A. Khan, X. Tang, C. Zhong, Q. Wang, S.-Y. Yang, F.-C. Kong, S. Yuan, A. S. D. Sandanayaka, C. Adachi, Z.-Q. Jiang, L.-S. Liao, *Adv. Funct. Mater.* **2021**, *31*, 2009488.

[8] H. L. Lee, W. J. Chung, J. Y. Lee, *Small* **2020**, *16*, 1907569.

[9] a) V. V. Patil, J. Lim, J. Y. Lee, *ACS Appl. Mater. Interfaces* **2021**, *13*, 12, 14440; b) V. V. Patil, H. L. Lee, I. Kim, K. H. Lee, W. J. Chung, J. Kim, S. Park, H. Choi, W.-J. Son, S. O. Jeon, J. Y. Lee, *Adv. Sci.* **2021**, *8*, 2101137; c) J. Hwang, C. W. Koh, J. M. Ha, H. Y. Woo, S. Park, M. J. Cho, D. H. Choi, *ACS Appl. Mater. Interfaces* **2021**, *13*, 51, 61454; d) V. V. Patil, K. H. Lee, J. Y. Lee, *J. Mater. Chem. C* **2020**, *8*, 8320.

[10] a) T. B. Nguyen, H. Nakanotani, T. Hatakeyama, C. Adachi, *Adv. Mater.* **2020**, *32*, 1906614; b) R. Niu, J. Li, D. Liu, R. Dong, W. Wei, H. Tian, C. Shi, *Dyes Pigm.* **2021**, *194*, 109581.

[11] X. Wu, B.-K. Su, D.-G. Chen, D. Liu, C.-C. Wu, Z.-X. Huang, T.-C. Lin, C.-H. Wu, M. Zhu, E. Y. Li, W.-Y. Hung, W. Zhu, P.-T. Chou, *Nat. Photonics* **2021,** *15***,** 780.

The CCDC depository number of ICZ-TAZ single crystal is 2181922.

10.1002/ange.202209425

Entry for the Table of Contents

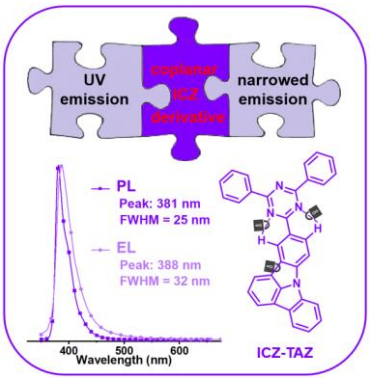

A coplanar strategy using indolo[3,2,1-*jk*]carbazole (ICZ) simultaneously achieves narrowed emission and ultraviolet (UV) emission in fluorescent organic light-emitting diodes (OLEDs), and a synthetic shortcut is carried out to efficiently obtain the target coplanar ICZ derivatives. 11-(4,6-diphenyl-1,3,5-triazin-2-yl)indolo[3,2,1-*jk*]carbazole (ICZ-TAZ) shows UV emission with peaks below 400 nm and narrowed full width at half maximum (FWHM) both in photoluminescence and electroluminescence, achieving best results among fluorescent UV-OLEDs.